NOTICE: this is the author’s version of a work that was accepted for publication in Organic Geochemistry. Changes resulting from the publishing process, such as peer review, editing, corrections, structural formatting, and other quality control mechanisms may not be reflected in this document. Changes may have been made to this work since it was submitted for publication. A definitive version was subsequently published in Organic Geochemistry, Vol. 69 (2014).
DOI: 10.1016/j.orggeochem.2014.01.013

Contrasting distributions of glycerol dialkyl glycerol tetraethers (GDGTs) in speleothems and associated soils

Alison J Blyth [a*], Catherine Jex [b,c], Andy Baker [b], Stuart Kahn [c], Stefan Schouten [d,e]

[a] *WA-OIGC, Department of Chemistry, Chemistry and Resources Precinct, Curtin University, GPO Box U1987, Perth, WA 6845, Australia*

[b] *Connected Waters Initiative Research Centre, University of New South Wales, Sydney 2052, Australia*

[c] *Water Research Centre, School of Civil and Environmental Engineering, University of New South Wales, Australia*

[d] *Department of Marine Organic Biogeochemistry, NIOZ Royal Netherlands Institute for Sea Research, 't Horntje, Texel, The Netherlands*

[e] *Department of Earth Sciences, Faculty of Geosciences, Utrecht University, Utrecht, The Netherlands*

*Corresponding author. Tel.: +61(0)892669388; fax: +61(0)892662300.
E mail address: alison.blyth@curtin.edu.au (A.J. Blyth).

ABSTRACT

Glycerol dialkyl glycerol tetraethers (GDGTs) preserved in speleothems can form useful records of terrestrial palaeotemperature. However, understanding of the sources of these compounds in caves is limited, particularly whether or not they should be considered as an in situ signal derived from microbial communities in the cave or vadose zone, a transported soil signal, or a mixture of the two. We have analysed speleothem samples and related soils from five cave sites and demonstrate that clear differences were apparent between soils and speleothems in GDGT distributions. Speleothems were primarily, but not uniformly, dominated by crenarchaeol, reflected in the Branched and Isoprenoid Tetraether (BIT) index values, and had a lower relative abundance of the crenarchaeol regioisomer than soils. The most distinct differences were in the bacterially derived branched GDGTs, where no relationship was seen between speleothems and soils for the Cyclisation of Branched Tetraethers (CBT) index, with speleothems in four out of five caves showing a higher degree of cyclisation in GDGT structures than could be explained by measured pH values. Differences in speleothem GDGT composition between sites were also seen. We suggest that the speleothem GDGT record is distinct from the GDGT distribution produced in soils, and is primarily derived from in situ microbial communities within the cave or vadose zone. Variation within these communities or in cave microenvironment also acts to produce site-specific differences.

Keywords

Speleothem; soil; temperature; pH; cave, microbe; GDGT; MBT; CBT; TEX_{86}

1. Introduction

Understanding past changes in our terrestrial environment, and especially identifying local and regional changes in continental temperature and the associated environmental response, is vital in understanding how our world will change in future. Speleothems (chemically precipitated cave deposits) are particularly well placed to provide such integrated terrestrial palaeoenvironmental records. They can be robustly dated, and contain a wealth of chemical signals, reflecting climate, for example, stable oxygen isotopes reflecting rainfall and fluctuations in global climate systems, (e.g. McDermott, 2004; Lachniet, 2009); and vegetation, for example, stable carbon isotopes of both the calcite and organic matter (e.g. Genty et al., 2003; Blyth et al., 2013), lipid biomarkers (e.g. Xie et al., 2003; Blyth et al., 2007, 2011), and lignin (Blyth & Watson 2009). Recent work has demonstrated that glycerol dialkyl glycerol tetraethers (GDGTs), compounds whose structure and composition in sedimentary records are known to relate to environmental parameters, and in particular, temperature (Schouten et al., 2013), are present in speleothems at recoverable levels (Yang et al., 2011; Blyth and Schouten, 2013). Two types of temperature proxy have been proposed using GDGTs, one using isoprenoid GDGTs (Fig. 1) derived from

aquatic archaea (e.g. TEX_{86} (TetraEther indeX of tetraethers consisting of 86 carbon atoms), Schouten et al., 2002) and one using branched GDGTs (Fig. 1) derived from bacteria in soils and other terrestrial environments (e.g. MBT/CBT (Methylation of Branched Tetraethers, and Cyclisation of Branched Tetraethers), Weijers et al., 2007). Generally, TEX_{86} has been applied to aquatic, in particular marine, settings, whilst the branched GDGTs have been associated with the terrestrial environment (reviewed by Schouten et al., 2013). For speleothems it has been shown that indices based on both branched and isoprenoid compound groups have a clear relationship with temperature (Blyth and Schouten, 2013). The use of a geographically diverse sample set to correlate speleothem GDGT composition with surface air temperature provided two speleothem-specific calibration equations (Blyth and Schouten, 2013), one for TEX_{86} (r^2 0.78, standard error of estimate ± 2.3 °C) and one for MBT/CBT (r^2 0.73, standard error of estimate ± 2.7 °C). It is therefore clear that speleothems have the potential to provide GDGT based palaeotemperature records.

A complicating factor identified by both Yang et al. (2011) and Blyth and Schouten (2013), is the difficulty in identifying the source environment of the GDGTs, with potential contributions from both in situ input from microbial communities in the cave and within the vadose zone of the overlying bedrock, and allochthonous input transported from the soil via infiltrating groundwater. The issue is of importance because the source of the compounds dictates which modern temperature measurements should

88 be used in future calibrations. If the compounds are primarily cave derived,
89 then the optimal calibration should be based on measured cave
90 temperatures. If they are soil derived, then they should be based on modern
91 surface or soil temperatures. At present, the published calibration equations
92 are based on surface air temperature as the values were available for the
93 largest data set, and mean annual surface temperature and cave air
94 temperature are considered to form a reasonable if not perfect
95 approximation. However, if the compounds could be shown to be primarily
96 in situ cave derived, then there would be a strong case for significantly
97 expanding the data set of available sites where modern calcite and
98 accurately measured cave temperatures can be obtained. Additionally, our
99 understanding of the more subtle relationships between the distributions of
100 GDGTs and environmental parameters is constantly evolving as increasing
101 numbers of studies are undertaken (e.g. Xie et al., 2012; Dirghangi et al.,
102 2013; Huguet et al., 2013). Increasing understanding of GDGT production in
103 cave and vadose zone environments and microenvironments should add to
104 the sum of this knowledge, especially if later combined with appropriate
105 microbiological research.

106 Clues about the origin of GDGTs in speleothems can be identified on
107 the basis of the composition of the GDGT signal. Blyth and Schouten (2013)
108 found that in most, but not all, samples, the speleothem GDGT signal was
109 dominated by crenarchaeol, a specific biomarker lipid for Thaumarchaeota,
110 whose presence in caves has been noted in DNA studies (Gonzalez et al.,

2006). Branched GDGTs formed a relatively minor component, in contrast to the distribution seen in most soils (Weijers et al., 2006; Schouten et al., 2013). Similarly, Yang et al., (2011) analysed soil, drip water and cave calcite samples from Heshang Cave in China, and found the cave signal (including speleothems, and surface cave bedrock samples) to be dominated by archaeal isoprenoid GDGTs, while the soil was dominated by bacterially derived branched GDGTs. Additionally, the internal composition of the isoprenoid and branched compound groups differed markedly between the soils and the calcite, lending credence to the idea of predominantly in situ GDGT production. However, to test the hypothesis of cave derived GDGTs more fully, it is necessary to look at paired soil and calcite samples from a broader range of geographical locations.

Here we have analysed the GDGTs present in soils recovered from above five caves in the UK and Australia, with a surface mean annual air temperature (MAT) range of 9 – 16 °C, and a surface mean annual precipitation (MAP) range of 617 – 1300 mm (Pooles Cavern, UK; Lower Balls Mine, UK; Wombeyan Caves, New South Wales, Australia; Gaden and Cathedral Caves, Wellington cave system, New South Wales, Australia). At least one speleothem from each of these caves has been previously analysed and included in the Blyth and Schouten (2013) calibrations, and the speleothems show a range of BIT (branched and isoprenoid tetraether index) values (0.05 – 0.69), indicating a varying degree of branched or isoprenoid compound dominance.

2. Material and method

2.1. Sites and samples

Table 1 lists the locations and environmental parameters for the five cave sites: Poole's Cavern (Derbyshire, UK) a shallow cave formed in Lower Carboniferous limestone, and overlain by woodland formed on abandoned lime kilns; Lower Balls Mine (Wiltshire, UK) a now abandoned limestone mine sunk into Middle Jurassic Oolites, and overlain by agricultural pasture (lower mine) and woodland (upper mine), with carbonaceous clayey soils; Wombyan Caves Reserve (New South Wales, Australia), a highly developed karst system formed in the high purity Wombeyan Marble unit in the Great Dividing Range, south-west of Sydney; and two caves at Wellington Caves Reserve (New South Wales, Australia), formed in the mixed thinly bedded and massive limestones of the Early Devonian Garra Formation. Speleothem GDGT data for these sites is taken from the sample set analysed in Blyth and Schouten (2013), and these sites were chosen in part because the speleothems are some of the guaranteed youngest in the sample set, providing closest comparability with the newly collected soils. The sample from Poole's Cavern was taken from regrowth on a stalagmite boss previously sampled in the late 1990s. At Wellington the samples were recently formed drip-straws and flowstones formed on man-made artefacts, and at Lower Balls Mine, where the speleothems are known to have a

maximum age of 100 years dating from the mine abandonment, the samples were thin and actively forming at collection. The sample from Wombeyan encompasses the last 40 years.

At each site a minimum of two soil samples were taken. Where contrasting vegetation or soil regimes were present over the cave (e.g. at Lower Balls Mine (LBM), where both woodland and agricultural grassland are present, and Pooles Cavern, where there is both a natural soil and soil developed over lime waste), a sample was taken from each regime. At all sites, the soil profile was thin, and the sample encompassed the whole available depth before the sampler hit either bedrock or rubble. All soils were analysed in replicate to take account of natural small scale heterogeneity.

2.2. Extraction

Speleothem samples were processed via acid digestion and liquid/liquid extraction, as described by Blyth and Schouten (2013). Soil samples were freeze-dried and aliquots of 1-10 g were crushed in a pestle and mortar. Samples from Pooles Cavern and LBM were extracted using 9:1 (v:v) dichloromethane (DCM)/ methanol (MeOH), at high temperature (100 ^{o}C) and pressure (7.6 x 10^{6} Pa) with a Dionex Accelerated Solvent Extractor (ASE) at NIOZ, while samples from Wombeyan and Wellington were extracted using a Dionex 150 ASE following the NIOZ methods at

UNSW. The extracts were dried under N_2, rediluted in DCM and separated into non-polar and polar fractions over activated Al_2O_3, eluted with DCM and 1:1 DCM/MeOH respectively. Samples Gad-soil-1 and Cat-soil-1 from above Gaden and Cathedral caves at Wellington were pre-filtered over dry $MgSO_4$ and cleaned cotton wool to remove excess particulates that otherwise blocked the Al_2O_3 column. The polar fraction was dried under N_2, rediluted in 99:1 (v/v) hexane/propanol, and filtered through a 0.45 µm PTFE filter (ø 4 mm).

Soil pH was measured at NIOZ (LBM and Poole's Cavern), and UNSW (Wombyean and Wellington). Briefly, an aliquot of crushed dry soil was suspended in deionised water at a ratio of 1 g soil:2.5 ml water, agitated for 5 min, and allowed to settle for 10 min. The pH was then measured using a calibrated probe (2 point calibration, standard solutions of pH 4 and 7) suspended in solution just above the surface of the soil. Measurements were performed in triplicate and averaged for each soil sample. WB-soil-2a was excluded from pH measurement due to lack of sample.

2.3. GDGT analysis

All analyses were undertaken at NIOZ in order to provide consistency with the previous speleothem analyses, and used the same analytical method as Blyth & Schouten (2013). Polar fractions were analysed for GDGTs using high performance liquid chromatography-atmospheric

pressure positive ion chemical ionization-mass spectrometry (HPLCAPCI-MS) following Schouten et al. (2007). HPLC-APCI-MS used an Agilent 1100 series LC with a Prevail Cyano column (2.1 x 150 mm, 3 μm; Alltech) maintained at 30 °C. GDGTs were eluted using a changing mixture of hexane and propanol as follows: 99% hexane/1% propanol (5 min), then a linear gradient to 1.8% propanol in 45 min. Flow rate was 0.2 ml/min. Single ion monitoring was set to scan the $[M+H]^+$ ions of the GDGTs with a dwell time of 237 ms for each ion. Only peaks with areas above 5000 were considered as being above the limit of quantitation (c.f. Schouten et al., 2007).

The following ratios were calculated (cren = crenarchaeol; cren' = crenarchaeol regio isomer):

Branched and Isoprenoid Tetraether index (Hopmans et al., 2004)

$$BIT = (III + II + I)/(Cren + III + II + I) \quad [1]$$

TetraEther indeX of tetraethers consisting of 86 carbon atoms (Schouten et al., 2002)

$$TEX_{86} = (2 + 3 + Cren')/(1 + 2 + 3 + Cren') \quad [2]$$

Methylation of branched tetraethers (Weijers et al., 2007)

$$MBT = (I + Ib + Ic)/(I + Ib + Ic + II + IIb + IIc + III + IIIb + IIIc) \quad [3]$$

226 Cyclisation of branched tetraethers (Weijers et al., 2007)

227 $CBT = -Log[(Ib + IIb)/(I + II)]$ [4]

228

229 Degree of cyclisation of branched tetraethers (closely related to CBT)

230 $DC = (Ib + Ic + IIb + IIc)/(2 \times I + 2 \times II)$ [5]

231

232 pH from CBT (Weijers et al., 2007)

233 $Calculated\ pH = (3.33 - CBT)/0.38$ [6]

234

235 **3. Results and discussion**

236

237 *3.1. GDGT composition*

238

239 All samples, with the exception of speleothem LBM-S3, contained
240 archaeal GDGTs 0, 1, 2, 3, crenarchaeol and the regio isomer of
241 crenarchaeol. LBM-S3 contained all of the above except for the regio isomer,
242 which was below the detection limit. For the branched GDGTs, speleothem
243 LBM-S3 was removed from the data set due to compound abundance being
244 below detection limits. All the other samples contained GDGT I, Ib, II, IIb,
245 IIc and III. GDGT Ic occurred in all samples except for speleothems LBM-S2
246 and PE-1. GDGT IIIb was detected in all samples except speleothem Wel-G-
247 1, while GDGT IIIc occurred in all speleothem and soil samples from Poole's
248 Cavern and LBM in the UK, but was only seen in two Australian samples –

249 a single soil replicate from Wombeyan (WB-soil-1bi), and speleothem Wel-C-
250 2.
251
252 *3.2. Variation in GDGT distribution between soils and speleothems*
253
254 Fig. 2 shows a ternary plot of crenarchaeol, GDGT 0 and the
255 combined branched GDGTs (I, II, III). Crenarchaeol is indicative of
256 Thaumarcheaota, while GDGT 0 (also known in the literature as
257 caldarchaeol) can be derived from Euryarchaeota including methanogenic
258 archaea, Crenarchaeota and Thaumarchaeota. A ratio value of GDGT 0 to
259 crenarchaeol > 2 has been proposed as a marker for methanogenic input
260 (Blaga et al., 2009). In the majority of samples crenarchaeol was
261 consistently the dominant isoprenoid compound. The only exception was
262 LBM-soil-1 where there was a high relative abundance of GDGT 0. LBM-
263 soil-1 had a GDGT 0/cren ratio of 9 – 11, in comparison to values of 0.1 – 0.5
264 for all the other soils as well as the speleothems. Similarly low values were
265 reported in other speleothems (Blyth and Schouten, 2013). This confirmed
266 that LBM-soil-1 was an outlier, with an abnormally high GDGT-0 input,
267 presumably due to highly localised methanogenic activity. Yang et al. (2012)
268 proposed an increase in GDGT 0 as a response to higher pH, but no
269 relationship between measured pH and relative abundance of GDGT 0 was
270 seen in the data here (r^2 0.00, data not shown), although it is worth noting
271 the range of measured pH was relatively limited.

The BIT index was originally designed to compare the input of bacterially derived branched GDGTs against crenarchaeol derived from Thaumarchaeota as a proxy for soil input to marine environments (Hopmans et al., 2004). Here we use it as a measure to compare the distribution of GDGTs in soils with that in speleothems. At Poole's Cavern, LBM and both Wellington sites, the speleothem BIT values were clearly lower than those for the corresponding soils, indicating lower comparative abundances of the branched tetraethers (Fig. 3). At Wombeyan, the difference was less marked, with WB-soil-1 in particular being very similar to the underlying speleothems. Recent studies have suggested that BIT values for soils may be affected by both pH and moisture, with more alkaline soils and drier soils showing lower values (Dirghangi et al., 2013; Yang et al., 2012). This has also been reflected in a broader isoprenoid / branched GDGT index using all GDGTs (Xie et al., 2012); however, no meaningful relationship was seen with any measured environmental parameter to explain the variation in this limited data set (pH r^2 0.01, p 0.94; surface MAP r^2 0.16, p 0.05; surface MAT r^2 0.13, p 0.13; data not shown).

Interestingly, whilst branched GDGTs were dominant in all the soils, the ternary plot and BIT values show that they also dominated in two speleothems – Pooles-1 and WM-4. The results suggest that, as indicated by the BIT results of Blyth and Schouten (2013), the crenarchaeol dominance seen by Yang et al., (2011) is site specific, and that the relative proportion of

the two groups of GDGTs in the speleothem bears no obvious relationship with that in the associated soils – e.g. the soil BIT values at Gaden Cave, Wellington were the second highest, whilst the underlying speleothem BIT was the lowest measured.

3.3. Variation in relative composition of isoprenoid tetraethers

To investigate the variation in compound relative abundance in the isoprenoid GDGTs, two measures were considered, TEX_{86}, and a principal components analysis (PCA) of the full compound distribution. For Wombeyan, Poole's Cavern and LBM, the speleothems showed a lower TEX_{86} value than the soils, while the samples from both Wellington caves were approximately in the same range as their associated soils (Fig. 4). The lower speleothem TEX_{86} values at Wombeyan, LBM and Poole's were primarily driven by a lower relative abundance of the crenarchaeol regio isomer (Table 2). A recent study of soil dwelling Thaumarchaeota showed that this isomer is produced in significant quantities in soils only where the I.1b subgroup of Thaumarchaeota are present (Sinninghe Damsté et al., 2012), suggesting that the difference seen here may reflect differences in the types of archeal communities present in some caves. Future microbiological and genetic studies are required to confirm this. However, despite the differences, both the speleothem and soil sample sets showed a good correlation between TEX_{86} and surface MAT (Fig 4.b; r^2 0.93, $p < 0.0001$ and

318 r^2 0.75, $p < 0.0001$, respectively), the soil data set showing higher TEX_{86}
319 values particularly at lower temperature. Similar inverse correlations were
320 seen between TEX_{86} and surface MAP (Fig. 4.c; speleothems, r^2 0.96, $p <$
321 0.0001; soils, r^2 0.67, $p < 0.0001$); however, as there is a clear inverse
322 relationship between temperature and rainfall at these sites, this would be
323 expected, and cannot be used to further extrapolate the role of rainfall in
324 GDGT distribution.

325 Two PCAs were run, one including all the isoprenoid GDGTs, and one
326 excluding GDGT 0 to avoid distortion from the LBM soil outliers for this
327 compound. Both indicate that the variation within the data could be
328 explained by a simple two component model (eigenvalues >1) and in both
329 cases the speleothems were separated from the soils. The loadings plots
330 indicate that this is a result of differences in the relative abundances of the
331 crenarchaeol regio isomer (PC-1) and of GDGTs 1, 2, and 3 (PC-2). Figure 5
332 shows the PCA excluding GDGT-0. The soils generally cluster around the
333 origin, with a tendency to score negatively on PC-1, while most of the
334 speleothems score positively on PC-1, but are split into two groups by PC-2.
335 The exception is Wel-G-1 which clusters with the soils from that site. The
336 division of the speleothems in PC-2 is driven by GDGTs 1, 2 and 3, with PE-
337 1 and the LBM speleothems having a higher relative abundance of GDGT-1
338 and a lower relative abundance of GDGT 3. This is not simply driven by the
339 differences in MAT between the UK and Australian sites since, using the
340 Blyth and Schouten (2013) calibration equations, LBM S-2 and S-3, WM-4,

and all Wellington speleothems showed TEX_{86} derived temperatures within the error of the calibration (generally within 1 °C of measured), while PE-1 under estimated the temperature by > 4 °C. Collectively, the distribution of the isoprenoid compounds indicate that speleothems and soils were generally distinct, possibly due to the types of Thaumarchaeota in the microbial community, but that there was an overall response to temperature, with some variation between different cave sites.

3.4. Variation in relative composition of branched tetraethers

Fig. 6 shows the scores and loadings plots for a PCA based on the relative abundances of the branched GDGTs. The variation is explained by a three component model (eigenvalues >1) and although the PCA did not show very distinct relationships between the compounds and groups of samples, it is clear from the loadings plots that certain compounds grouped consistently as might be expected (e.g. I and II; Ib and Ic; IIIb, and IIIc) and that some compounds did influence certain sample scores (e.g the score for WM-4 appeared to have a consistent relationship with GDGT III). Some consistent trends can also be seen in the grouping of soils and speleothems. All the Australian soils and Pooles-soil-1 cluster together on PC-2 and 3. On PC-1 there is some separation between the Wellington soils, and the Wombeyan soils, the latter of which cluster with Pooles-soil-1. However, they all have negative scores compared with the speleothems. Only the LBM soils cluster

364 differently, having positive scores on PC1 and 3, and slightly negative on
365 PC-2. The speleothems are distinct from the soils (with the exception of the
366 soils from LBM), being largely positive on PC-1. However, they show much
367 greater scatter, indicating variable relationships with different compounds.
368 As GDGT IIIc was only present at two sites, a second PCA was run with this
369 compound removed, but the results were broadly the same.

370 To investigate the role of cyclisation and degree of methyl branching
371 in distinguishing between samples, Figs. 7 and 8 show plots of the MBT
372 index (the degree of methylation, believed to be influenced by pH and
373 temperature; Weijers et al., 2007) and the CBT and DC ratios, depicting the
374 degree of cyclization (influenced by pH). MBT', as defined by Peterse et al.
375 (2012), excluding IIIb and IIIc, was calculated for the sample set but, as the
376 resulting values were within 0.01 of MBT, we used the Weijers et al. (2007)
377 equation to maintain consistency with Blyth and Schouten (2013).

378 The results show that the speleothems at LBM and Cathedral Cave,
379 Wellington were within the same range of MBT values as their overlying
380 soils, but that at Wombeyan Caves, the speleothem had a lower MBT (e.g. a
381 greater relative abundance of branched GDGTs) and at Gaden Cave,
382 Wellington, Wel-G-1 had a distinctly higher MBT than related soils. At
383 Poole's Cavern, the speleothem was broadly similar to Pooles-soil-2, but
384 much lower than Pooles-soil-1. When correlated against environmental
385 parameters, MBT in the soils showed a better relationship with MAT than
386 the speleothems (soils, r^2 0.75, $p < 0.0001$; speleothems, r^2 0.63, p 0.03. Fig.

387 7b), while no relationship between MBT and pH was apparent (Fig 7c.).
388 Both groups had an inverse correlation with MAP, although as noted above
389 this is most likely due to the relationship between MAT and MAP at these
390 sites.

391 The CBT and DC ratios of the speleothems were distinct from the
392 soils at all sites (Fig. 8a,b). For Wombeyan, Wellington and LBM, the
393 speleothems had a lower CBT/higher DC (i.e. more compounds with
394 cylcopentane moieties) than their related soils. The reverse was the case for
395 Poole's Cavern. Fig. 9 shows the calculated pH based on the CBT values
396 (following Weijers et al., 2007), against measured pH for the soils and drip
397 water. For the soils, all the Australian sites showed a good match between
398 measured and calculated pH, while Poole's Cavern and LBM soils had a
399 higher calculated pH than the measured values. In the speleothems, the
400 CBT proxy consistently overestimated pH, except for PE-1 from Poole's
401 Cavern, where there is a very high drip water pH, which was substantially
402 underestimated by the calculated value. The general overestimation of pH
403 vs. drip water values may simply be due to the fact we were perforce using a
404 soil-derived equation (Weijers et al., 2007) to estimate pH in a speleothem
405 context – a speleothem specific CBT - pH calibration needs to be developed
406 in future to test this. Another possibility is that the drip-water pH sampling
407 is not fully representative of longer term variations in the cave water pH
408 that might occur during speleothem formation. The finding from PE-1 is in
409 line with work from lakes and soils, which found that at high pH levels

above 7.5 -8.5, the relationship between CBT and pH breaks down (Xie et al., 2012; Schoon et al., 2013), possibly due to differences in the proton gradients within the cell membranes in high pH environments. Nonetheless, excluding Poole's Cavern, there were marked differences between the CBT and DC values of the soils on the one hand and speleothems on the other which were not reflected in the measured pH values. This was especially noticeable at the Wellington Caves sites where the drip water and soil pH values were within error of each other, but the CBT and DC of the speleothems against the soils were very clearly distinct. This suggests that additional parameters, tending towards increasing the relative abundance of cyclic moieties within branched GDGTs, act on the speleothem signal.

4. Conclusions

The results clearly show that there are substantial differences between GDGT distributions in soils and speleothems. Fig. 10 shows a summary graph plotting soils against speleothems for the major GDGT parameters. Some relationship is apparent in TEX_{86} and MBT, although in both cases the range of values in the speleothem samples is greater than that in the corresponding soils. Neither BIT or CBT show any relationship between the two groups. In some cases, the results show similarities in the GDGT signals at a specific site. However, in no case does this extend across all the measured parameters (e.g. Wel-G-1 has an isoprenoid GDGT

composition similar to that for the Wellington soils, but the branched GDGT composition is markedly different). We therefore conclude that there is clear evidence that the dominant sources of GDGTs in speleothems result from in situ production within either the cave or the overlying vadose zone and, whilst we do not rule out some soil derived input to the signal, this appears to be a minor component of the overall speleothem GDGT record. We suggest that the relationships between soils and speleothems (e.g. in TEX_{86}, and to a lesser extent MBT) are due to parallel response to the same environmental parameter, most likely temperature in this case, rather than a common GDGT source. To enhance understanding of the speleothem GDGT signal further, future work is indicated in three directions: further in-depth studies of specific sites to identify where in the cave/bedrock the primary source is located; combined geochemical and microbiological studies of modern cave environments to establish the degree of variation within and between cave sites and the relationship with environmental parameters; lastly, the collection of an increased modern speleothem sample set from sites with monitored cave temperatures in order to refine the speleothem TEX_{86} and MBT/CBT calibrations for use in palaeoenvironmental research.

Acknowledgements

The study was funded by ARC Discovery Project DP110102124 (A.B., S.K., A.J.B. and C.J.) and an AINSE Research Fellowship to A.J.B., who also acknowledges a Leverhulme Early Career Fellowship in support of the

speleothem analyses. S.S thanks the Netherlands Organisation for Scientific Research (NWO) for financial support through a VICI grant. J. Ossebaar, E. Hopmans and A. Mets (NIOZ) are thanked for assistance. J. MacDonald of the University of Newcastle, NSW supplied WM-4 and assisted in soil sample collection, A. Hartland, then of the University of Birmingham supplied PE-1. A. Walker, general manager of Poole's Cavern, is thanked for assistance with soil sample collection and site access. Speleothem samples LBM-S2 and LBM-S3 were supplied by D. Dominguez-Villar, while J. Dredge of the University of Birmingham assisted with soil sample collection. The support of Wellington Council is acknowledged for access and sampling at Wellington Caves.

References

Blaga, C.I., Reichart, G.J., Heiri, O., Sinninghe Damsté, J.S., 2009. Tetraether membrane lipid distributions in water column particulate matter and sediments: a study of 47 European lakes along a north-south transect. Journal of Palaeolimnology 41, 523-540.

Blyth, A.J., Watson J.S., 2009 Thermochemolysis of organic matter preserved in stalagmites: a preliminary study. Organic Geochemistry 40, 1029-1031.

Blyth, A.J., Schouten, S., 2013. Calibrating the glycerol dialkyl glycerol tetraether signal in speleothems. Geochimica et Cosmochimica Acta 109, 312 – 328.

Blyth, A.J., Asrat, A., Baker, A., Gulliver, P., Leng, M., Genty, D. 2007. A new approach to detecting vegetation and land-use change: high resolution lipid biomarker records in stalagmites. Quaternary Research 68, 314-324.

Blyth, A.J., Baker, A., Thomas, L.E., van Calsteren, P., 2011. A 2000-year lipid biomarker record preserved in a stalagmite from northwest Scotland. Journal of Quaternary Science 26, 326-334.

Blyth, A.J., Smith, C.I., Drysdale, R.N. 2013 A new perspective on the $\delta^{13}C$ signal preserved in speleothems using LC-IRMS analysis of bulk organic matter and compound specific stable isotope analysis. Quaternary Science Reviews 75, 143-149.

Dirghangi, S.S., Pagani, M.., Hren, M.T., Tipple, B.J., 2013. Distribution of glycerol dialkyl glycerol tetraethers in soils from two environmental transects in the USA. Organic Geochemistry 59, 49-60.

Genty, D., Blamart, D., Ouahdi, R., Gilmour, M., Baker, A., Jouzel, J., Van-Exter, S. 2003. Precise dating of Dansgaard-Oeschger climate oscillations in western Europe from stalagmite data. Nature 421, 833-837.

Gonzalez J.M., Portillo M.C., Saiz-Jimenez C., 2006. Metabolically active Crenarchaeota in Altamira Cave. Naturwissenschaften 93, 42-45.

Hartland, A., Fairchild, I.J., Lead, J.R., Zhang, H., Baalousha, M., 2011. Size, speciation and lability of NOM-metal complexes in hyperalkaline cave dripwater. Geochimica et Cosmochimica Acta 75, 7533-7551.

500 Hartland, A., Fairchild, I.J., Lead, J.R., Borsato, A., Baker, A., Frisia, S.,
501 Baalousha, M., 2012. From soil to cave: transport of trace metals by natural
502 organic matter in karst dripwaters. Chemical Geology 304-305, 68-82.
503 Hopmans, E.C., Weijers, J.W.H., Schefuß, E., Herfort, L., Sinninghe
504 Damsté, J.S., Schouten, S., 2004. A novel proxy for terrestrial organic
505 matter in sediments based on branched and isoprenoid tetraether lipids.
506 Earth and Planetary Science Letters 224, 107-116.
507 Huguet, A., Fosse, C., Laggoun-Défarge, F., Delarue, F., Derenne, S. 2013.
508 Effects of a short-term experimental microclimate warming on the
509 abundance and distribution of branched GDGTs in a French peatland.
510 Geochimica et Cosmochimica Acta 105, 294-315.
511 Lachniet, M.S., 2009. Climatic and environmental controls on speleothem
512 oxygen-isotope values, Quaternary Science Reviews 28, 412-432
513 McDermott, F., 2004. Palaeo-climate reconstruction from stable isotope
514 variations in speleothems: a review. Quaternary Science Reviews 23, 901-
515 918.
516 McDonald, J., Drysdale, R., Hill, D., Chisari, R., Wong, H., 2007. The
517 hydrochemical response of cave drip waters to sub-annual and inter-annual
518 climate variability, Wombeyan Caves, SE Australia. Chemical Geology 244,
519 605-623.
520 Peterse F., van der Meer J., Schouten S., Weijers J.W.H., Fierer N., Jackson
521 R.B., Kim J.-K., Sinninghe Damsté J.S., 2012. Revised calibration of the

522 MBT-CBT paleotemperature proxy based on branched tetraether membrane
523 lipids in surface soils. Geochimica et Cosmochimica Acta 96, 215-229.
524 Schoon, P.L., de Kluijver, A., Middelburd, J.J., Downing, J.A., Sinninghe
525 Damsté, J.S., Schouten, S., 2013. Influence of lake water pH and alkalinity
526 on the distribution of core and intact polar branched glycerol dialkyl glycerol
527 tetraethers (GDGTs) in lakes. Organic Geochemistry 60, 72-82.
528 Schouten, S., Hopmans, E.C., Schefuß, E., Sinnginghe Damsté, J.S., 2002.
529 Distributional variations in marine crenarchaeotal membrane lipids: a new
530 tool for reconstructing ancient sea water temperatures? Earth and
531 Planetary Science Letters 204, 265-274.
532 Schouten, S., Huguet, C., Hopmans, E.C., Sinninghe Damsté, J.S., 2007.
533 Improved analytical methodology of the TEX_{86} paleothermometry by high
534 performance liquid chromatography/atmospheric pressure chemical
535 ionization-mass spectrometry. Analytical Chemistry 79, 2940-2944.
536 Schouten, S., Hopmans, E.C., Sinninghe Damsté, J.S., 2013. The organic
537 geochemistry of glycerol dialkyl glycerol tetraether lipids: a review. Organic
538 Geochemistry 54, 19-61.
539 Sinninghe Damsté, J.S. Rijpstra, W.I.C., Hopmans, E.C., Jung, M-Y., Kim,
540 J-G., Rhee, S-K., Stieglmeier, M., Schleper, C., 2012. Intact and core glycerol
541 dibiphytanyl glycerol tetraether lipids of Group I.1a and I.1b
542 *Thaumarchaeota* in soil. Applied and Environmental Microbiology 78, 6866-
543 6874.

544 Weijers, J.W.H., Schouten, S., Spaargaren, O.C., Sininghe Damsté, J.S.,
545 2006. Occurrence and distribution of tetraether membrane lipids in soils:
546 implications for the use of the TEX_{86} proxy and the BIT index. Organic
547 Geochemistry 37, 1680-1693.
548 Xie, S., Yi, Y., Huang, J., Hu, C., Cai, Y., Collins, M., Baker, A. 2003. Lipid
549 distribution in a subtropical southern China stalagmite as a record of soil
550 ecosystem response to palaeoclimate change. Quaternary Research 60, 340-
551 347.
552 Xie, S., Pancost, R.D., Chen, L., Evershed, R.P., Yang, H., Zhang, K., Huang,
553 J., Xu, Y. 2012. Microbial lipid records of highly alkaline deposits and
554 enhanced aridity associated with significant uplift of the Tibetan Plateau in
555 the Late Miocene. Geology 40, 291-294.
556 Yang, H., Ding, W., Zhang, C.L., Wu, X., Ma, X., He, G., Huang, J., Xie, S.,
557 2011. Occurrence of tetraether lipids in stalagmites: implications for
558 sources and GDGT-based proxies. Organic Geochemistry 42, 108-115.
559 Yang, H., Ding, W., Wang, J., Jin, C., He, G., Qin, Y., Xie, S., 2012. Soil pH
560 impact on microbial tetraether lipids and terrestrial input index (BIT) in
561 China. Science China Earth Sciences 55, 236-245.
562

563 **Table and figure captions**

564 **Table 1.**

565 Location and environmental details for samples.

566 **Table 2.**

567 Relative abundance of isoprenoid GDGTs, normalised to total isoprenoid
568 GDGTs and total isoprenoid GDGTs excluding GDGT 0 (speleothem
569 samples are marked in italics).
570 **Fig. 1.** Structures for the isoprenoid and branched GDGTs.
571 **Fig. 2.** Ternary plot of relative abundances of GDGT 0, crenarchaeol and
572 summed branched GDGTs (GDGT I, II, III).
573 **Fig. 3.** BIT index for the speleothem and soil samples. No relationship is
574 apparent between the soil and speleothem values for each site.
575 **Fig. 4.** a) TEX_{86} in speleothem and soil samples; b) relationship between
576 TEX_{86} and surface MAT; and c) the relationship between TEX86 and surface
577 MAP in the speleothems and soils respectively.
578 **Fig. 5.** a) PCA scores plot for isoprenoid GDGTs showing separation of
579 samples on two components; b) PCA plot showing loadings for isoprenoid
580 compounds. This analysis was run with GDGT 0 excluded due to distorting
581 methanogenic input to LBM soils.
582 **Fig. 6.** a) PCA scores plots for a 3 component model for branched GDGTs; b)
583 loadings plot of PC-1 vs. PC-3; c) loadings plot for PC-2 vs. PC-3
584 **Fig. 7.** a) MBT for speleothem and soil samples; b) relationships in the two
585 groups between MBT and MAT, showing a stronger correlation for the soil
586 data set; c) relationship between MBT and pH showing no correlation. The
587 regression line for the speleothems was not included as it was distorted by
588 the abnormally high drip water value at Poole's Cavern.

589 **Fig. 8.** a) CBT for speleothem and soil samples; b) DC for speleothem and
590 soil samples. PE-1 shows an opposite response to the rest of the speleothem
591 samples.
592 **Fig. 9.** Measured vs. calculated (Eq. 6) pH, with the dotted line indicating
593 1:1. PE-1 forms a clear outlier, consistent with the relationship between
594 CBT and pH breaking down at high pH levels, as observed for lakes (Schoon
595 et al., 2013). Slight overestimation of pH in the other speleothems may
596 result from the use of a soil calibrated equation.
597 **Fig 10.** Scatter plots comparing average speleothem and soil GDGT
598 parameters for each site. a) BIT; b) TEX_{86}; c) CBT (triangle represents
599 Poole's Cavern which has been excluded from this regression due to the
600 abnormal drip-water pH); d) MBT.

Table 1

Sample	Type	Location	Soil pH	Drip water pH [b]	Surface MAT °C [c]	MAP mm [d]
PE-1[a]	Stalagmite	Pooles Cavern, England	-	11.7 ± 0.4		
PC-soil-1	Soil (top 10 cm)	Pooles, natural soil above cave, adjacent to lime spoil heap	6.4	-	9	1300
PC-soil-2	Soil (top 10 cm)	Pooles, soil from lime soil heap above cave	7.8	-		
LBM-S2	Stalagmites	Lower Balls Mine (LBM), England	-	8		
LBM-S3				8		
LBM-soil-1	Soil (top 10 cm)	LBM, thin soil under light woodland, over limestone. Outside upper entrance to mine	7.6	-	10	995
LBM-soil-2	Soil (top 10 cm)	LBM, soil under agricultural grassland above mine, halfway between upper and lower entrances	7.5	-		
WM-4	Stalagmite	Wombeyan Caves, New South Wales, Australia	-	7.6 ± 0.4		
WB-soil-1a	Soil (0-2 cm)	Wombeyan, above caves, very thin soil under open woodland	8.0	-	13.7	804
WB-soil-1b	Soil (2-5 cm)		8.2	-		
WB-soil-2a	Soil (0-2 cm)		-	-		
WB-soil-2b	Soil (2-5 cm)		8.0	-		
Wel-C-1	Straw	Cathedral Cave, Wellington, NSW, Australia	-	7.7 ± 0.5		
Wel-C-2	Flowstone			7.7 ± 0.5		
Wel-C-3	Flowstone on bottle			7.7 ± 0.5		
Cat-soil-1	Soil (top 20 cm)	Wellington, above Cathedral Cave, degraded box grass woodland, with bare soil and sparse tree cover	7.5	-	16	617
Cat-soil-2	Soil (top 20 cm)		7.3	-		
Wel-G-1	Straw	Gaden Cave, Wellington NSW, Australia	-	7.7 ± 0.5		
Gad-soil-1	Soil (top 20 cm)	Wellington, above Gaden Cave, box grass woodland, not degraded.	7.3	-		
Gad-soil-2	Soil (top 20 cm)		7.8	-		

[a] PC-1 in Blyth and Schouten, 2013; [b] Drip water pH taken from: Poole's Cavern, Hartland et al., 2011; LBM, I. Fairchild personal communication; Wombeyan, McDonald et al. 2007; Wellington, Martin Andersen, Nerilee Edwards personal communication; [c] surface MAT as reported by Blyth and Schouten, 2013; [d] surface mean annual rainfall: Poole's Cavern and LBM, Hartland et al 2012; Wellington and Wombeyan data from the Australian Government Bureau of Meteorology.

Table 2.

Sample	Isoprenoid GDGTs (%)						Isoprenoid GDGTs (%;GDGT 0 excluded)				
	GDGT 0	GDGT 1	GDGT 2	GDGT 3	Cren	Cren isomer	GDGT 1	GDGT 2	GDGT 3	Cren	Cren isomer
PE-1	*17.7*	*21.4*	*10.2*	*2.0*	*48.1*	*0.6*	*26.0*	*12.4*	*2.4*	*58.5*	*0.7*
PC-soil-1	16.9	9.5	7.6	3.9	59.8	2.4	11.4	9.1	4.7	71.9	2.9
PC-soil-2	16.8	10.1	9.8	4.7	56.5	2.2	12.1	11.7	5.7	67.9	2.6
LBM-S2	*24.4*	*12.6*	*7.2*	*3.4*	*52.4*	*0.0*	*16.6*	*9.6*	*4.5*	*69.3*	*0.0*
LBM-S3	*17.1*	*18.1*	*16.0*	*3.7*	*44.2*	*0.8*	*21.9*	*19.3*	*4.5*	*53.4*	*1.0*
LBM-soil-1	88.5	1.2	1.0	0.4	8.6	0.3	10.8	8.7	3.8	74.3	2.4
LBM-soil-2	21.7	6.2	5.3	3.4	60.2	3.2	7.9	6.8	4.4	76.8	4.1
WM-4	*12.8*	*14.9*	*11.4*	*12.2*	*47.6*	*1.3*	*17.1*	*13.0*	*13.9*	*54.5*	*1.4*
WB-soil-1a	14.0	6.3	6.5	4.0	62.4	6.8	7.3	7.5	4.7	72.5	7.9
WB-soil-1b	10.2	5.7	6.6	4.2	65.4	7.9	6.3	7.3	4.7	72.9	8.8
WB-soil-2a	10.4	7.3	7.4	3.8	63.3	7.7	8.2	8.2	4.2	70.7	8.6
WB-soil-2b	9.5	7.0	7.6	3.7	64.0	8.1	7.8	8.4	4.1	70.8	8.9
Wel-C-1	*8.9*	*11.0*	*10.7*	*11.9*	*55.7*	*1.8*	*12.1*	*11.8*	*13.1*	*61.1*	*2.0*
Wel-C-2	*8.0*	*9.6*	*9.8*	*10.8*	*58.2*	*3.7*	*10.4*	*10.7*	*11.7*	*63.2*	*4.0*
Wel-C-3	*8.8*	*9.9*	*10.1*	*12.1*	*56.6*	*2.6*	*10.9*	*11.0*	*13.3*	*62.0*	*2.9*
Cat-soil-1	15.0	8.3	10.9	4.1	57.2	4.5	9.8	12.8	4.8	67.4	5.2
Cat-soil-2	22.1	4.7	7.7	4.3	53.3	7.9	6.0	9.8	5.6	68.4	10.1
Wel-G-1	*6.9*	*7.3*	*6.0*	*8.7*	*63.8*	*7.3*	*7.9*	*6.5*	*9.4*	*68.5*	*7.8*
Gad-soil-1	15.4	7.8	10.4	4.5	55.5	6.5	9.2	12.3	5.3	65.6	7.6
Gad-soil-2	13.0	7.2	11.2	5.3	56.2	7.2	8.3	12.8	6.0	64.6	8.3

Fig. 1

Isoprenoid GDGTs

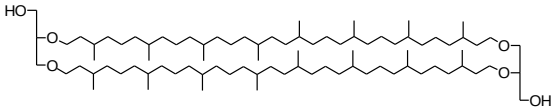

GDGT-0

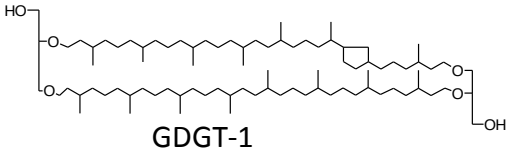

GDGT-1

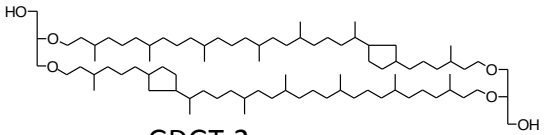

GDGT-2

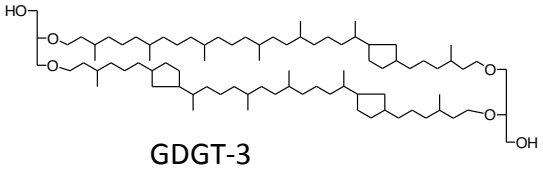

GDGT-3

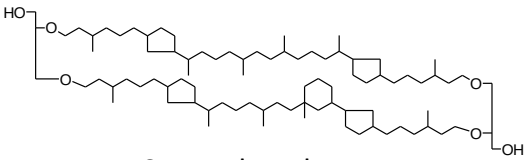

Crenarchaeol

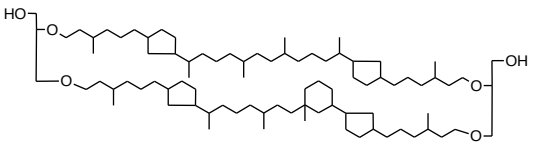

Crenarchaeol regio-isomer

Branched GDGTs

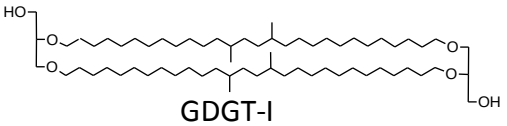

GDGT-I

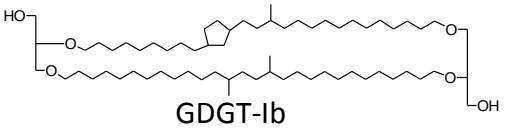

GDGT-Ib

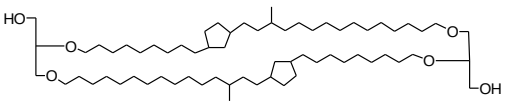

GDGT-Ic

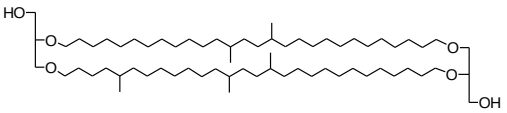

GDGT-II

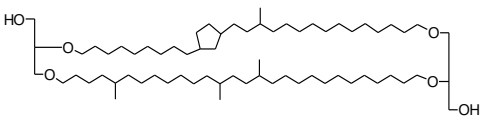

GDGT-IIb

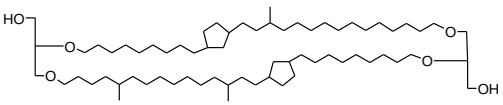

GDGT-IIc

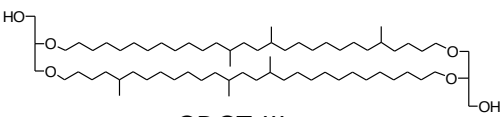

GDGT-III

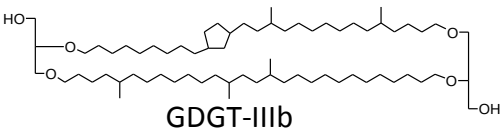

GDGT-IIIb

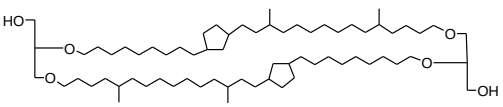

GDGT-IIIc

Isoprenoid GDGTs:
GDGT 0: m/z 1302 GDGT 1: m/z 1300
GDGT 2: m/z 1298 GDGT 3: m/z 1296
Crenachaeol: m/z 1292

Branched GDGTs:
GDGT I: m/z 1022 Ib: m/z 1020 Ic: m/z 1018
GDGT II: m/z 1036 IIb: m/z 1034 IIc: m/z 1032
GDGT III: m/z 1050 IIIb: m/z 1048 IIIc: m/z 1046

Fig. 2

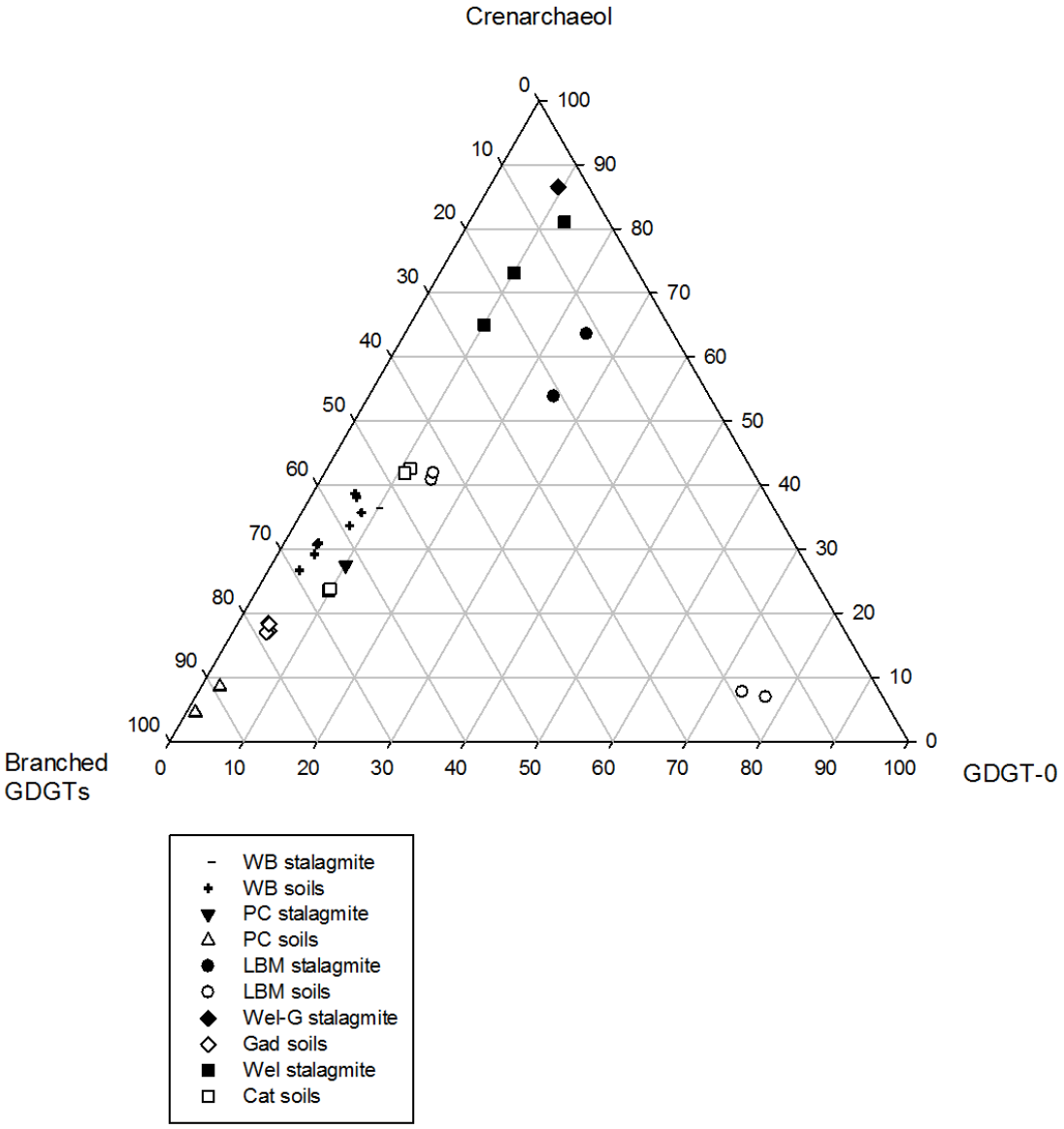
Crenarchaeol
Branched GDGTs
GDGT-0
0
10
20
30
40
50
60
70
80
90
100
WB stalagmite
WB soils
PC stalagmite
PC soils
LBM stalagmite
LBM soils
Wel-G stalagmite
Gad soils
Wel stalagmite
Cat soils

Fig. 3

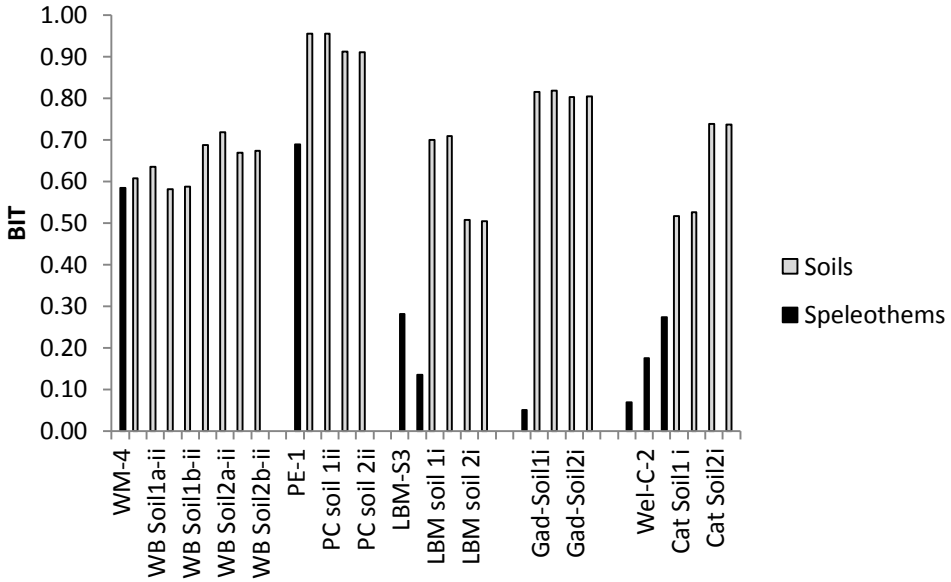
BIT
1.00
0.90
0.80
0.70
0.60
0.50
0.40
0.30
0.20
0.10
0.00
WM-4
WB Soil1a-ii
WB Soil1b-ii
WB Soil2a-ii
WB Soil2b-ii
PE-1
PC soil 1ii
PC soil 2ii
LBM-S3
LBM soil 1i
LBM soil 2i
Gad-Soil1i
Gad-Soil2i
Wel-C-2
Cat Soil1 i
Cat Soil2i
Soils
Speleothems

Fig. 4

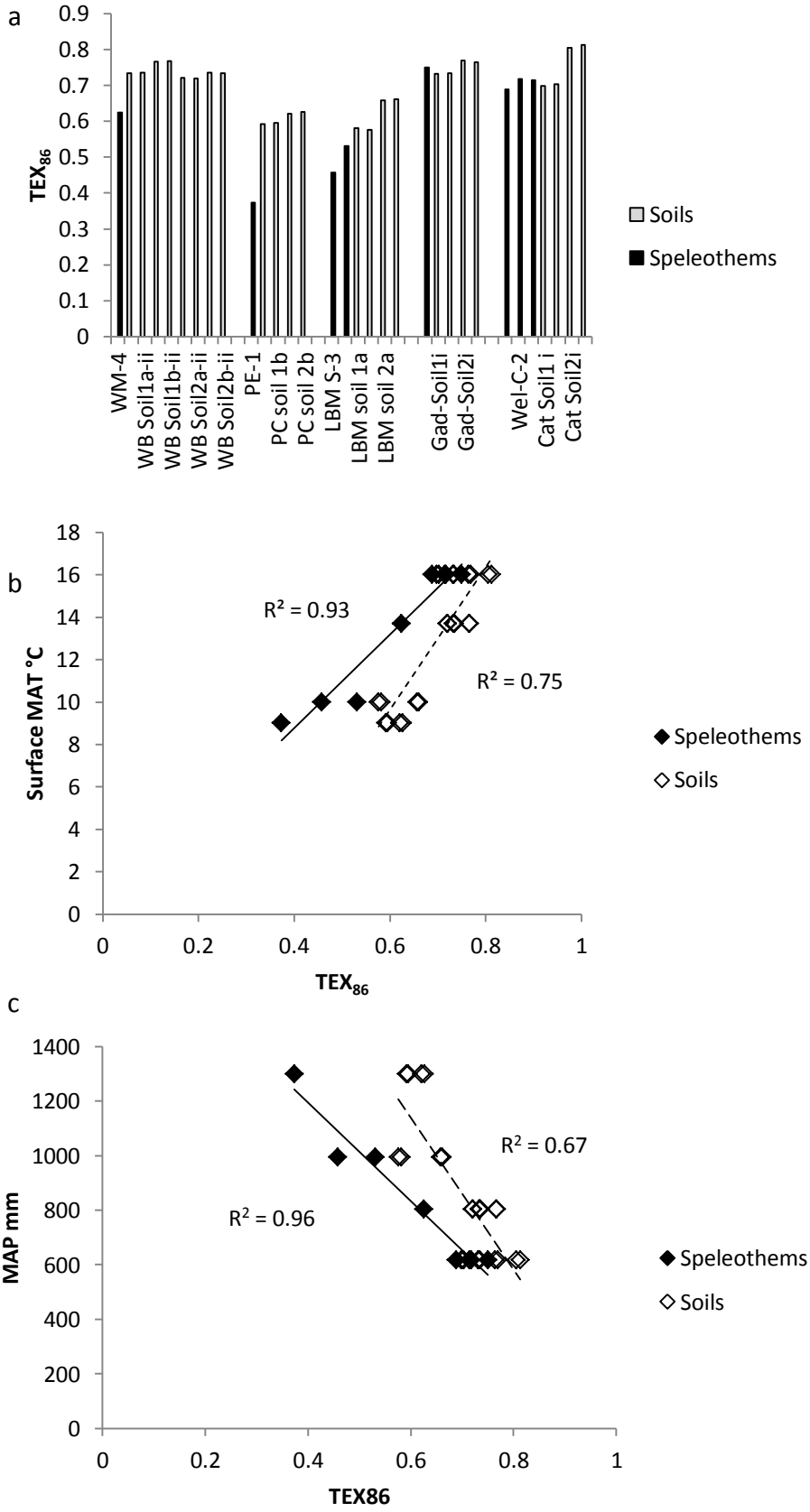
a
TEX86
0.9
0.8
0.7
0.6
0.5
0.4
0.3
0.2
0.1
0
WM-4
WB Soil1a-ii
WB Soil1b-ii
WB Soil2a-ii
WB Soil2b-ii
PE-1
PC soil 1b
PC soil 2b
LBM S-3
LBM soil 1a
LBM soil 2a
Gad-Soil1i
Gad-Soil2i
Wel-C-2
Cat Soil1 i
Cat Soil2i
Soils
Speleothems
b
Surface MAT °C
18
16
14
12
10
8
6
4
2
0
R² = 0.93
R² = 0.75
0
0.2
0.4
0.6
0.8
1
TEX86
Speleothems
Soils
c
MAP mm
1400
1200
1000
800
600
400
200
0
R² = 0.67
R² = 0.96
0
0.2
0.4
0.6
0.8
1
TEX86
Speleothems
Soils

Fig. 5

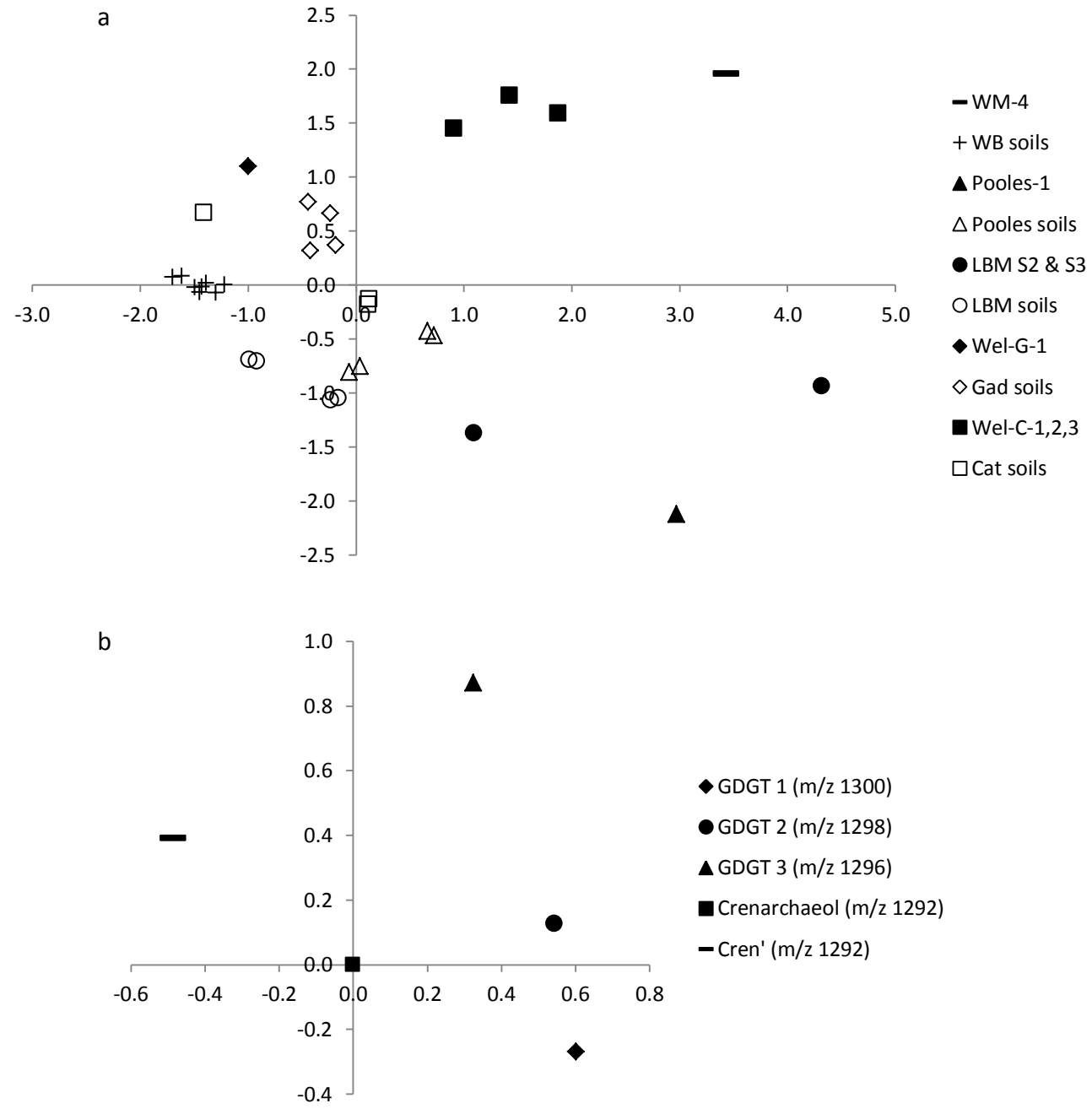
a
2.5
2.0
1.5
1.0
0.5
0.0
-0.5
-1.0
-1.5
-2.0
-2.5
-3.0
-2.0
-1.0
0.0
1.0
2.0
3.0
4.0
5.0
WM-4
WB soils
Pooles-1
Pooles soils
LBM S2 & S3
LBM soils
Wel-G-1
Gad soils
Wel-C-1,2,3
Cat soils
b
1.0
0.8
0.6
0.4
0.2
0.0
-0.2
-0.4
-0.6
-0.4
-0.2
0.0
0.2
0.4
0.6
0.8
GDGT 1 (m/z 1300)
GDGT 2 (m/z 1298)
GDGT 3 (m/z 1296)
Crenarchaeol (m/z 1292)
Cren' (m/z 1292)

Fig. 6

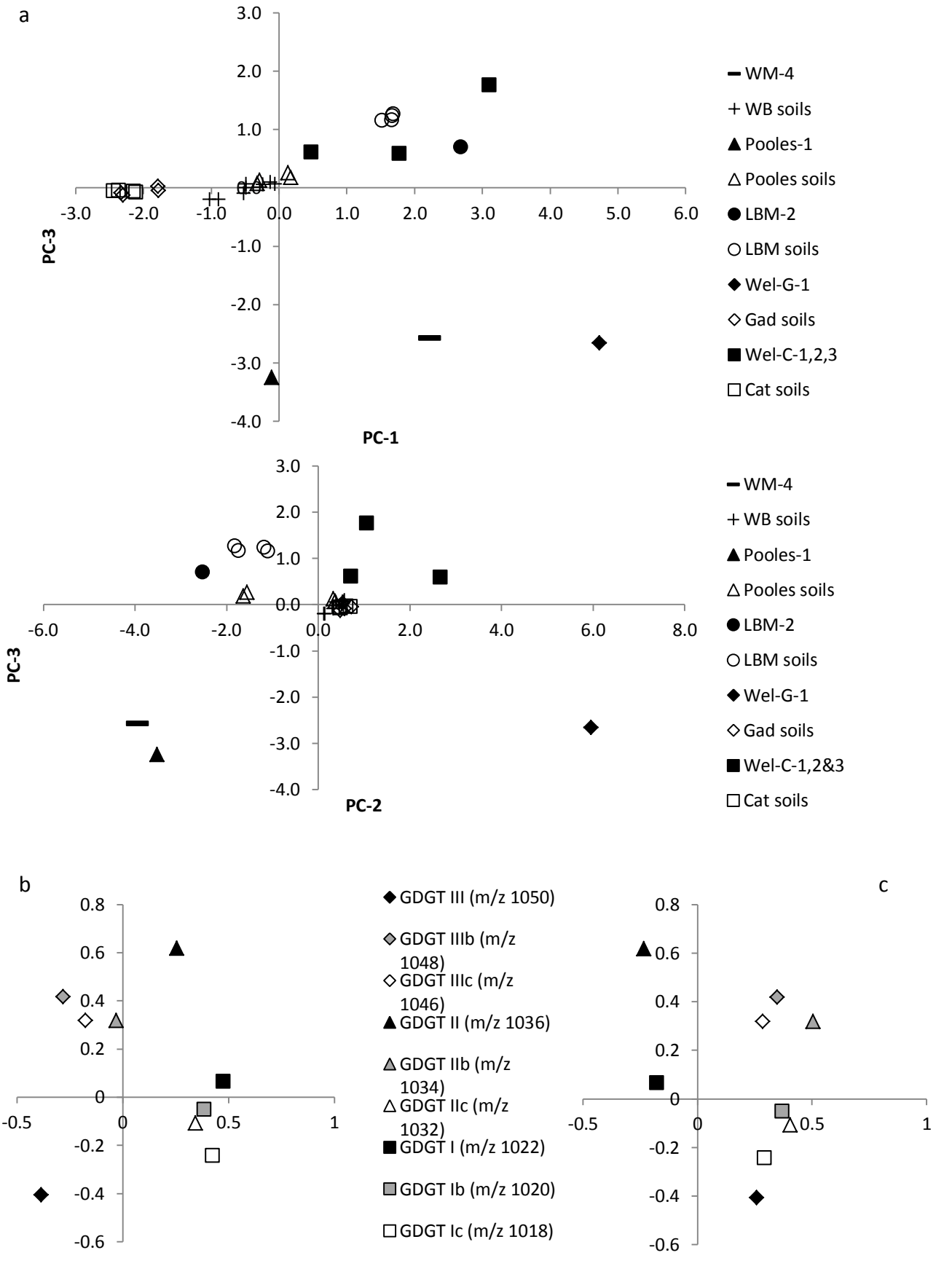
a
PC-3
PC-1
PC-2
WM-4
WB soils
Pooles-1
Pooles soils
LBM-2
LBM soils
Wel-G-1
Gad soils
Wel-C-1,2,3
Wel-C-1,2&3
Cat soils
b
c
GDGT III (m/z 1050)
GDGT IIIb (m/z 1048)
GDGT IIIc (m/z 1046)
GDGT II (m/z 1036)
GDGT IIb (m/z 1034)
GDGT IIc (m/z 1032)
GDGT I (m/z 1022)
GDGT Ib (m/z 1020)
GDGT Ic (m/z 1018)

Fig. 7

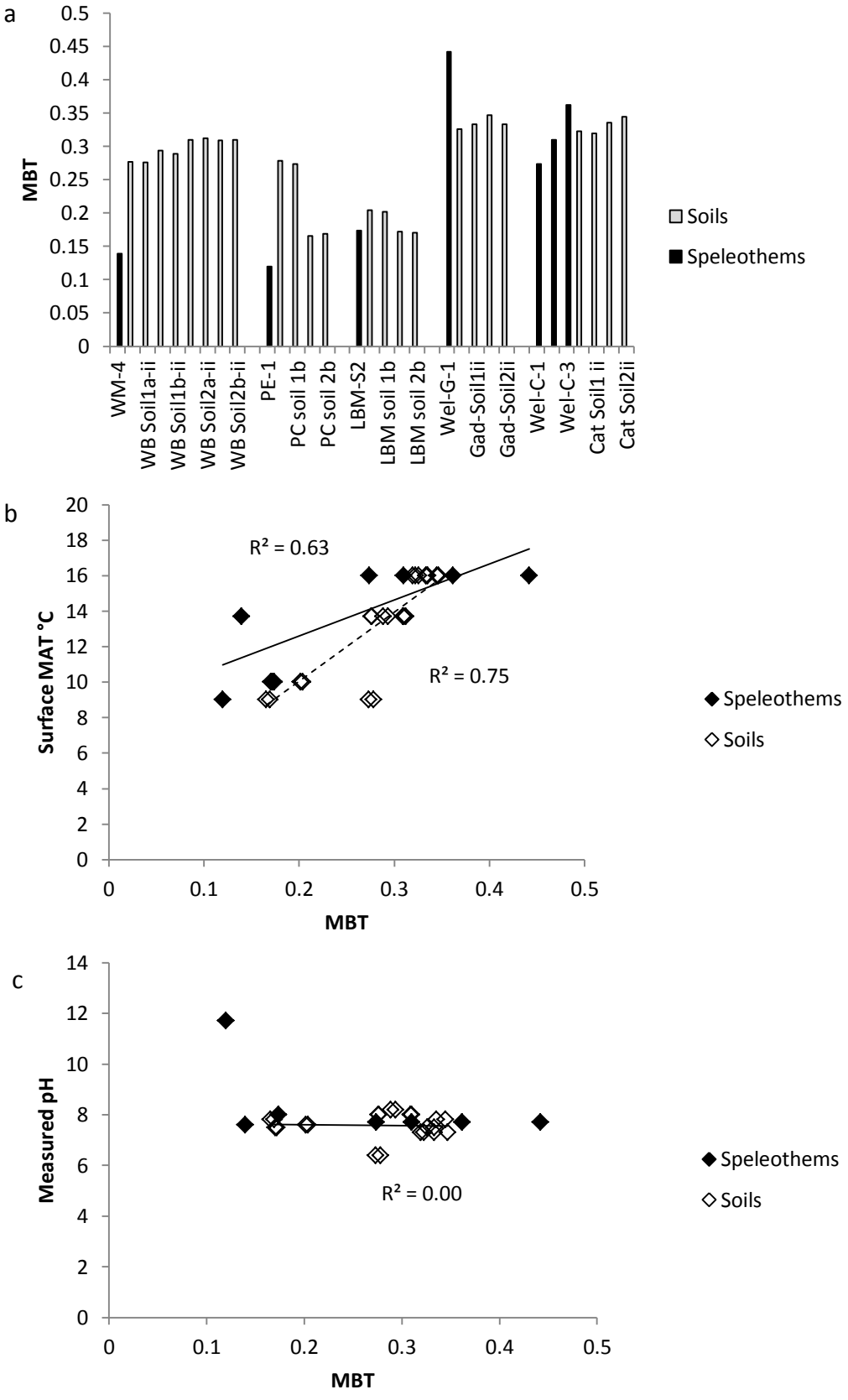
a
MBT
0
0.05
0.1
0.15
0.2
0.25
0.3
0.35
0.4
0.45
0.5
WM-4
WB Soil1a-ii
WB Soil1b-ii
WB Soil2a-ii
WB Soil2b-ii
PE-1
PC soil 1b
PC soil 2b
LBM-S2
LBM soil 1b
LBM soil 2b
Wel-G-1
Gad-Soil1ii
Gad-Soil2ii
Wel-C-1
Wel-C-3
Cat Soil1 ii
Cat Soil2ii
Soils
Speleothems
b
Surface MAT °C
MBT
R² = 0.63
R² = 0.75
Speleothems
Soils
c
Measured pH
MBT
R² = 0.00
Speleothems
Soils

Fig. 8

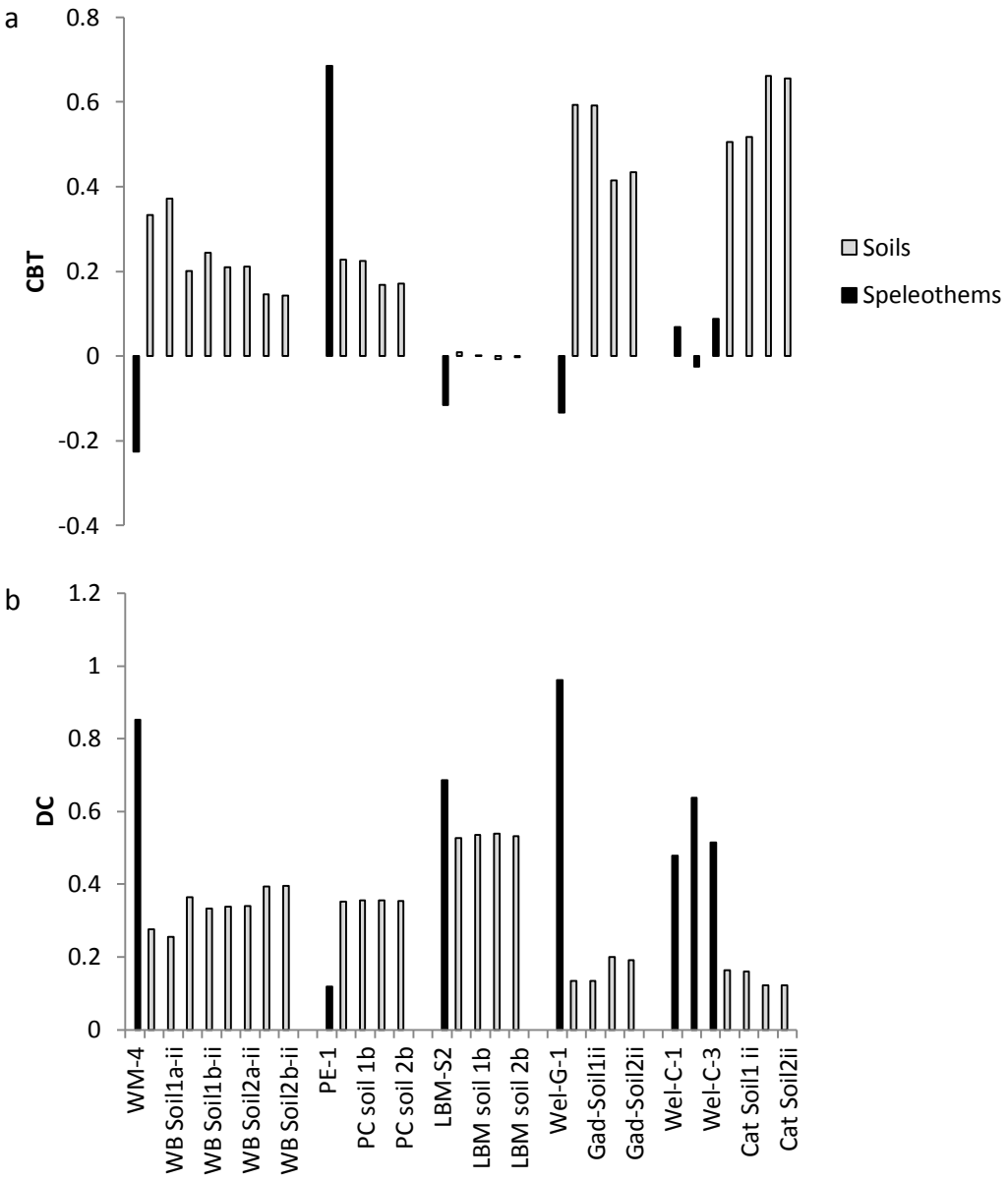
a
0.8
0.6
0.4
0.2
0
-0.2
-0.4
CBT
Soils
Speleothems
b
1.2
1
0.8
0.6
0.4
0.2
0
DC
WM-4
WB Soil1a-ii
WB Soil1b-ii
WB Soil2a-ii
WB Soil2b-ii
PE-1
PC soil 1b
PC soil 2b
LBM-S2
LBM soil 1b
LBM soil 2b
Wel-G-1
Gad-Soil1ii
Gad-Soil2ii
Wel-C-1
Wel-C-3
Cat Soil1 ii
Cat Soil2ii

Fig. 9

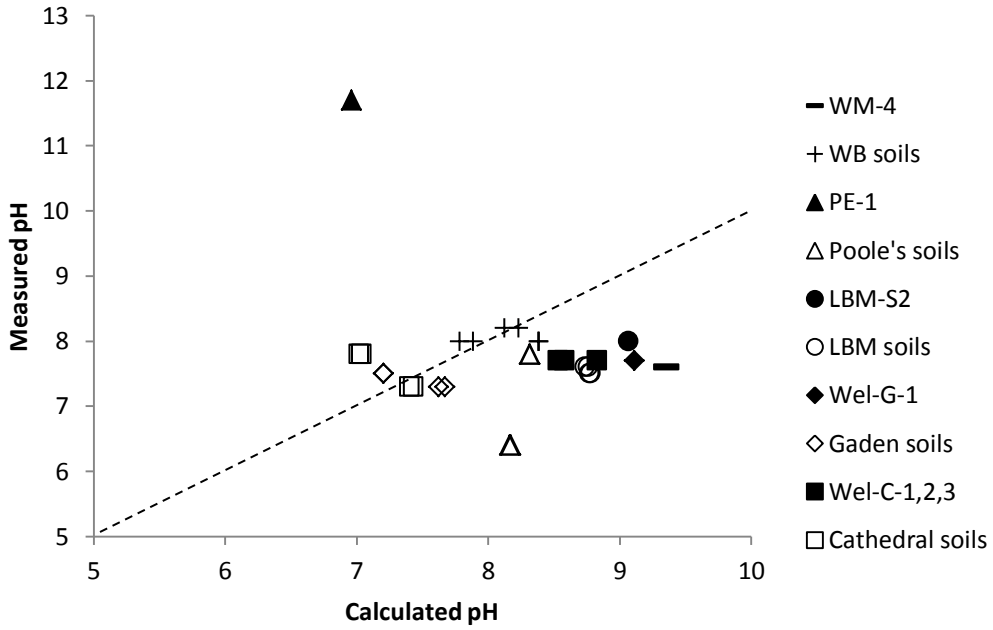
13
12
11
10
9
8
7
6
5
Measured pH
5
6
7
8
9
10
Calculated pH
WM-4
WB soils
PE-1
Poole's soils
LBM-S2
LBM soils
Wel-G-1
Gaden soils
Wel-C-1,2,3
Cathedral soils

Fig. 10

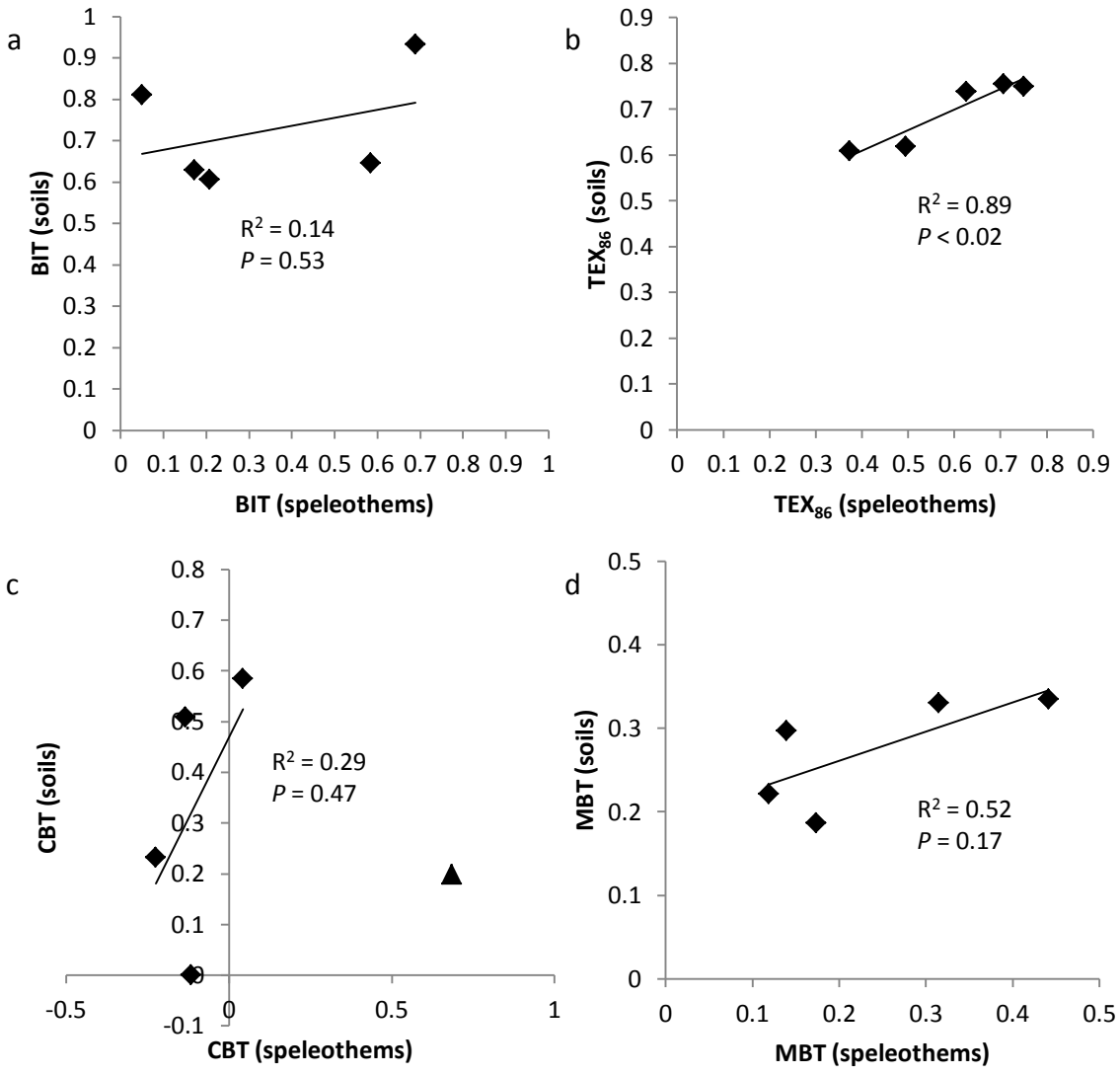
a
BIT (soils)
BIT (speleothems)
R2 = 0.14
P = 0.53
b
TEX86 (soils)
TEX86 (speleothems)
R2 = 0.89
P < 0.02
c
CBT (soils)
CBT (speleothems)
R2 = 0.29
P = 0.47
d
MBT (soils)
MBT (speleothems)
R2 = 0.52
P = 0.17